Molecular Physics, Vol. 103, Nos. 21–23, 10 November–10 December 2005, 2851–2861

Taylor & Francis
Taylor & Francis Group

Monte Carlo simulation of the electric double layer: dielectric boundaries and the effects of induced charge

DOUGLAS HENDERSON*†, DIRK GILLESPIE‡, TÍMEA NAGY§ and DEZSÖ BODA§

†Department of Chemistry and Biochemistry, Brigham Young University, Provo Utah 84602, USA
‡Department of Molecular Biophysics and Physiology, Rush University Medical Center, Chicago, Illinois 60612, USA
§Department of Physical Chemistry, University of Veszprém, H-8201 Veszprém, P.O. Box 158, Hungary

(*Received 28 January 2005; in final form 11 March 2005*)

To model the double layer near an electrode, theories and simulations must include the different dielectric coefficients of the electrode, the commonly-postulated 'inner' layer, and the electrolyte. Recently, Boda *et al*. [D. Boda, D. Henderson, K.-Y. Chan, D.T. Wasan. *Phys. Rev*. E, **69**, 046702, (2004)] developed a technique to include inhomogeneous dielectric coefficients in arbitrary geometries in a simulation. Here, Monte Carlo simulation results based on this method are reported for the density profiles of 1:1, 2:2 and 2:1 aqueous electrolytes. The simulations include two dielectric boundaries, one from an inner layer of low dielectric coefficient and one from an uncharged metal electrode. In addition, an extension of a Poisson–Boltzmann (PB) type theory due to Onsager and Samara [L. Onsager, N.N.T. Samara. *J. chem*. Phys., **2**, 528, (1934)] is developed and compared with our simulation results. This approach works best for 1:1 salts at low concentrations.

1. Introduction

The authors are delighted to join the editors in dedicating this paper and issue to Ben Widom in recognition of his important contributions to chemical physics. We insert this paper into this special issue to commemorate the Widom insertion method. Ben is an exemplary scientist and person and a good friend. We wish him many more productive years.

The common theory of electrochemical interfaces is the Poisson–Boltzmann (PB) type theory of Gouy and Chapman (GC) [1, 2]. In the GC theory, the ions are point charges, the solvent is a dielectric continuum with a dielectric coefficient ϵ and the electrode is a flat surface with uniform surface charge. In simulations, ions can be modelled as charged, hard spheres (the *primitive model*, PM). No matter what theory or simulation method is used, however, to bring results of the primitive model into agreement with experiments, it is necessary—or at least sufficient—to postulate an interfacial region or 'inner' layer (also called a Helmholtz or Stern layer) of some thickness δ in which the dielectric coefficient ϵ^* is smaller than that of the bulk electrolyte. Any treatment of the double layer for this primitive model thus includes at least three regions with differing dielectric coefficients: the electrode, the inner layer and the bulk (often called the diffuse layer). At each of the two dielectric interfaces, Poisson's equation predicts a surface charge that is a function of the location of all ions. Moreover, each surface charge affects the other surface charge, thereby coupling the different layers of dielectrics.

The GC theory assumes that the capacitance of the interfacial electrolyte is that of two independent capacitors in series. The capacitor representing the diffuse layer is calculated from the GC theory without reference to the inner layer. The inner layer capacitance is then computed and the two capacitances are added in series. The unstated, but very real, assumption is that the diffuse layer density, charge and potential profiles are completely unchanged by the presence of different dielectric coefficients in the inner layer and in the electrode. In effect, the inner and diffuse layer capacitors are considered to be electrostatically decoupled (or at most loosely coupled), an assumption that has not been tested. One goal of this work is to examine this assumption.

These simplifications mean that analytic results can be obtained even if the electrode charge is large. The widespread use of this theory results from an understandable preference for the convenience of an analytical theory. However, the GC theory is not very accurate. An empirical choice for ϵ^* and δ only conceals this fact.

*Corresponding author. Email: doug@chem.byu.edu

Molecular Physics
ISSN 0026–8976 print/ISSN 1362–3028 online © 2005 Taylor & Francis
http://www.tandf.co.uk/journals
DOI: 10.1080/00268970500108668

Even if one obtains a reasonable fit for the capacitance, this means only that the experimental potential at the electrode, which is known anyway, has been reproduced. There is no reason to believe that the potential away from the electrode, say that of an ion at its distance of closest approach (at the edge of the inner layer) is accurate (see figure 5 of Schmickler and Henderson [3] for evidence that it is not).

The simulations of Torrie and co-workers [4–7] are widely interpreted as validating the GC theory. At best, however, these simulations show the GC theory to give reasonably good values for the density profiles of 1:1 aqueous electrolytes when dielectric inhomogeneities are ignored, when the ions that do not have too large a diameter, and only when the theory is used for the same electrode *charge* as that of the simulation. Errors in the GC theory are apparent for divalent ions, for ions with a large diameter, for solvents with a lower dielectric coefficient [8] (or equivalently, a lower temperature), and when the GC theory is used with the same electrode *potential* (rather than the same electrode charge) as the simulation [9, 10]. See, in particular, figure 2 (*a*) and (*b*) and figure 4 (*a*) and (*b*) of [9], where the GC counterion profiles are considerably smaller than the simulation results when the potential is used as the independent variable. For a 1:1 salt, the counterion profile is in fairly reasonable agreement with simulation only when the electrode charge is used as the independent variable. This point has been overlooked and is nontrivial given the large errors in the potential–charge curve predicted by the GC theory and that the potential is the more natural variable in the GC theory (and experiments). For 2:2 and 2:1 salts, the agreement with simulations is poor whether potential or charge is used as the independent variable.

Even for 1:1 aqueous electrolytes with smaller size ions, most of the Torrie–Valleau simulations do not address the question of the reliability of the underlying model of a continuum dielectric representation of the solvent and an absence of any dielectric boundaries. They do report one set of simulations [5] for the case when the dielectric coefficient of the electrode differs from that of the electrolyte, leading to induced charge on the electrode, but they do not consider an inner layer with a different dielectric coefficient. This is because they were able to treat only a single dielectric boundary by means of electrostatic images. Since they do not consider an inner layer with a different dielectric coefficient, the issue of whether a dielectric boundary at the inner–diffuse layer interface has an effect on the diffuse layer profiles did not arise in their investigation.

In this paper, we investigate by simulation the consequences of an inhomogeneous dielectric coefficient and, in particular, consider the effects of an inner layer on the diffuse layer. In addition, we solve Poisson's equation for a system with two planar dielectric interfaces and use this result to develop an extension of inhomogeneous PB theory of Onsager and Samara [11] for an electrolyte near a planar dielectric boundary for the case of two planar dielectric boundaries. As one might expect on the basis of past experience with the PB theories, this approach is most useful for a 1:1 salt at low concentrations. Even so, it provides valuable insight into the simulation results.

Since the effect of dielectric discontinuities is likely to be most apparent for uncharged electrodes, in this initial paper we confine our attention to uncharged electrodes. Charged electrodes will be considered later.

2. Model

Our model electrolyte is the *restricted* primitive model (RPM), where the ions are charged hard spheres, all with the same diameter. In this paper, we use, $d = 3$ Å. That is, the direct interaction between the ions can be characterized by the energy,

$$W_e = \frac{1}{2}\sum_i z_i e \psi_e(\mathbf{r}_i), \tag{1}$$

where z_i is the valence of the ith ion, e is the magnitude of the electronic charge, and

$$\psi_e(\mathbf{r}_i) = \begin{cases} \displaystyle\sum_{j\neq i} \frac{z_j e}{\epsilon_j |\mathbf{r}_i - \mathbf{r}_j|}, & \text{for } |\mathbf{r}_i - \mathbf{r}_j| \geq d, \\ \infty, & \text{for } |\mathbf{r}_i - \mathbf{r}_j| < d \end{cases} \tag{2}$$

is the potential raised by the ions at $\mathbf{r}_i$. In equation (2), ϵ_j is the dielectric coefficient of the region where the jth ion resides. The charge of an ion is assumed to be located at the centre of the ion. As is pointed out below, the centres of the ions are always located in the region whose dielectric coefficient is ϵ_3, therefore $\epsilon_j = \epsilon_3$ in equation (2). It is assumed that the interior of an ion has the same dielectric coefficient as the solvent. Thus, we need not worry about induced charge on the surface of an ion. In principle, such induced charge could be included and might yield interesting results but this would make the simulation very time consuming, perhaps impossibly so. We will return to this point in section 3.

Space is divided into three regions of dielectric coefficients ϵ_1, ϵ_2 and ϵ_3, as shown in figure 1. The electrode occupies region 1 ($x < 0$) and contains no ions. We assume that the electrode is a metal whose surface is planar and smooth. Thus, the dielectric coefficient in this region is $\epsilon_1 = \infty$. Region 2 is the inner layer

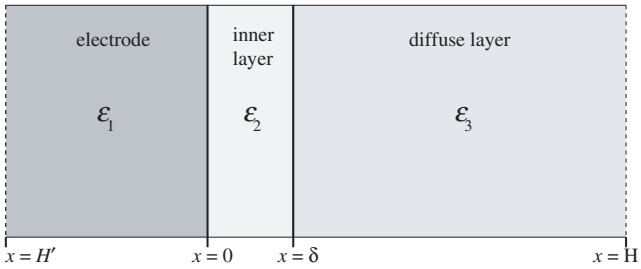

Figure 1. Simulation geometry. The cell consists of three regions, the electrode, $H' < x < 0$, whose dielectric coefficient is ϵ_1, the inner layer, $0 < x < \delta$, whose dielectric coefficient is ϵ_2, and the diffuse layer and bulk, $\delta < x < H$, whose dielectric coefficient is ϵ_3.

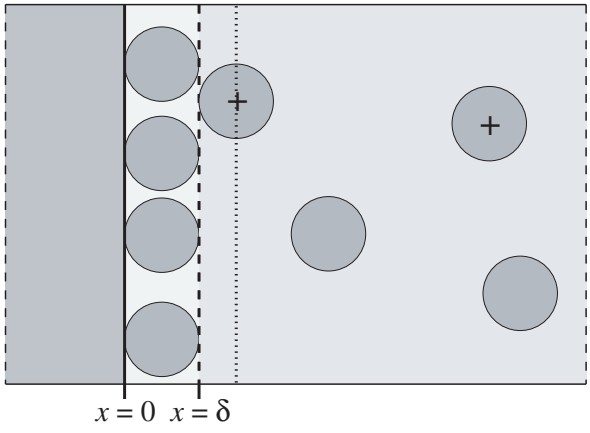

Figure 2. Inner and diffuse layer models. The inner layer is presumed to be inaccessible to the ions. For example, it could consist of a solvation layer of water molecules. Note that the ions are always located in the region of the dielectric coefficient ϵ_3.

$(0 < x < \delta)$. We assume that the inner layer contains no ions but consists of a layer of solvent molecules that solvate the electrode. For simplicity, the solvent molecules are assumed to have a diameter d equal to the ion diameter ($\delta = d$). As is seen in figure 2, the distance of closest approach of an ion centre to the electrode is $d + (d/2) = 3d/2$. The charge of an ion is never closer than $d/2$ to the inner–diffuse layer dielectric boundary and is always in a homogeneous dielectric. In our method, the charge on the dielectric boundary is a set of discretized charged surface elements. Because the dielectric interfaces are hard walls for the ions, an ion whose interior has a dielectric coefficient ϵ_3 does not overlap with the inner layer of dielectric coefficient ϵ_2. Consequently, new dielectric boundaries do not appear during the simulation.

The dielectric coefficient of the inner layer is assumed to be $\epsilon_2 = \epsilon^* = 6$. The ions are confined to the third layer, region 3 ($x > \delta$). The dielectric coefficient of this diffuse layer is assumed to be that of the solvent and is taken to be $\epsilon_3 = \epsilon = 80$. This is slightly higher than that of water and higher yet than that of a 1 M aqueous solution. However, the precise value of ϵ is unimportant for the moment; we are interested in whether the dielectric boundaries affect the diffuse layer profiles. This question is independent of ϵ.

In this study we used a coupling constant, $q^{*2} = e^2/\epsilon_3 dk_B T = 2.32$ (k_B and T are Boltzmann's constant and the temperature), which corresponds to monovalent ions of diameter 3 Å in an solvent of dielectric coefficient 80 at room temperature.

3. Simulation method

Our method is that of Boda *et al*. [12], which is an extension of the work of Allen *et al*. [13]. If we characterize the inhomogeneous dielectric by a space dependent dielectric coefficient $\epsilon(\mathbf{r})$, then polarization charge is induced at a dielectric interface. If the dielectric boundaries are sharp, the polarization charge is a surface charge that we denote by $h(\mathbf{r})$. Allen *et al*. have introduced a functional $I[h(\mathbf{r})]$ that is a function of $h(\mathbf{r})$ for a given configuration of the source charges (the ions). They have shown that the induced charge that minimizes the functional is a solution of the Poisson equation.

In our previous work [12], we have developed a different solution for this variational problem. The result is an integral equation whose discretization results in a matrix equation. If we assume that the source charges are ions as described in the previous section and that the dielectric boundaries are sharp, the following equation can be written

$$\int_B h(\mathbf{r}')\left[\epsilon(\mathbf{r}')\delta(\mathbf{r}-\mathbf{r}') + \Delta\epsilon(\mathbf{r})\frac{(\mathbf{r}-\mathbf{r}')\cdot\mathbf{n}(\mathbf{r})}{|\mathbf{r}-\mathbf{r}'|^3}\right]\mathrm{d}\mathbf{r}' = \Delta\epsilon(\mathbf{r})\nabla\psi_e(\mathbf{r})\cdot\mathbf{n}(\mathbf{r}), \quad (3)$$

where the dielectric coefficient on the boundary $\epsilon(\mathbf{r})$ is defined to be the arithmetic mean of the two dielectric coefficients on each side of the boundary. Furthermore, the dielectric discontinuity $\Delta\epsilon(\mathbf{r})$ is the difference of the two dielectric coefficients on each side of the boundary in the direction of the local unit normal of the surface $\mathbf{n}(\mathbf{r})$. The integral is taken over the dielectric boundary surfaces $\mathcal{B}$, $\delta(\mathbf{r}-\mathbf{r}')$ is the Dirac delta and $\psi_e(\mathbf{r})$ is the potential of the source charges defined in equation (2). After discretizing $\mathbf{r}$ into discrete values $\mathbf{r}_i$ by dividing the surface $\mathcal{B}$ into small surface elements $\mathcal{B}_i$, $\mathbf{r}_i$ being the centre of the ith surface element, a matrix equation is obtained

$$A\mathbf{h} = \mathbf{c}, \quad (4)$$

where the vectors **h** and **c** contain the discretized values of the induced charge and the right-hand side of equation (3) at the discretized values of $\mathbf{r}_i$, respectively. The matrix is constructed from the expression in square brackets in the integrand:

$$A_{ij} = \epsilon(\mathbf{r}_i)\delta_{ij} + \Delta\epsilon(\mathbf{r}_i)\int_{B_j} \frac{(\mathbf{r}_i - \mathbf{r}')\cdot \mathbf{n}(\mathbf{r}_i)}{|\mathbf{r}_i - \mathbf{r}'|^3}\, \mathrm{d}\mathbf{r}'. \qquad (5)$$

It is seen that the matrix depends only on the geometry of the inhomogeneous dielectric, and it does not depend on the source charges. It is the vector **c** that depends on the positions of the source charges. Therefore, the matrix need be inverted only once at the beginning of the simulation provided that the geometry does not change during the simulation. (This is the reason for the definition of the ions in the preceding section: when a dielectric boundary appears or moves, the matrix should be reinverted, a very time consuming process.) In a MC step, the vector **c** is changed, from which the induced charge can be calculated from the matrix multiplication $\mathbf{h} = A^{-1}\mathbf{c}$. The potential produced by the induced charges is

$$\psi_i(\mathbf{r}) = \sum_j \frac{h_j a_j}{|\mathbf{r} - \mathbf{r}_j|}, \qquad (6)$$

where h_j and a_j are the charge density and the area of the jth surface element, respectively. When calculating the energy of the system, which is an essential step in a MC simulation, the interaction energy between the ith source charge and the induced charges

$$W_i = \frac{1}{2}\sum_i z_i e \psi_i(\mathbf{r}_i) \qquad (7)$$

should be added to W_e (equation (1)). The computational cell is bounded by hard reflecting walls at $x = -H'$ and $x = H$. The precise value of H' is unimportant since there are no ions in the electrode. To avoid unwanted dielectric boundaries at $x = H'$ and $x = H$, we assume that the dielectric coefficient is ϵ_1 for $x < H'$ and ϵ_3 for $x > H$. The metal surface is assumed to be located at $x = 0$. Periodic boundary conditions are applied in the lateral (y, z) directions. The width of the cell in lateral directions is given by L. The values of L and H vary with the ion concentration and are greater the lower the concentration.

An important aspect of the simulation is the discretization of the surface charge, namely, the construction of the grid on the surface. For the simulation cell used in this work, the grid is rectangular due to the periodic boundary conditions in the y and z directions. The width of the surface element square is $\Delta x = d$ because we have shown that this grid resolution yields satisfactory results if the ions move in the region of higher dielectric coefficient [12].

Equation (3) is general in the sense that the method can be applied to curved surfaces or to dielectric boundaries that are in close proximity, but we must evaluate the matrix with much more care. This matrix formulation has been used in quantum mechanical solvation programs based on apparent surface charges [14] first introduced by Hoshi *et al*. [15], although our derivation and resulting formulas are more general. After this work was completed, it was found that Green and Lu have performed MC simulations to study polarization effects using this matrix equation to study polarization effects in biological ion channels [16–18].

In our simulations we have used an NVT ensemble. The $L \times H$ dimensions of our cell are $20d \times 184d$, $21.7d \times 26d$, and $15d \times 21d$ for concentrations 0.05, 0.5 and 2 M, respectively. The number of ions are 120, 200 and 300 for these concentrations. We averaged over 115 000–500 000 MC cycles depending on concentration. No long range corrections were used in this work because in [12] we have shown that for uncharged surfaces and for the range of parameters that we consider here, the cell dimensions that we have used are large enough.

4. Simulation results

We report results for an uncharged electrode for four different models, with different values for the dielectric coefficient in the three regions. We adopt the notation $\epsilon_1|\epsilon_2|\epsilon_3$ to describe a particular model. The simplest is Model 80|80|80, the model that underlies the GC theory, where the dielectric medium is homogeneous. The second is Model ∞|80|80, where the electrode is a metal but the inner layer has the same dielectric coefficient as the diffuse layer, and the third model is Model ∞|6|80, where the inner and diffuse layer dielectric coefficients differ. Finally, we consider briefly the Model 6|6|80.

Results for 1:1 electrolytes are reported in figures 3–5 for the cases where the bulk concentrations are $c(\infty) = 0.05$, 0.5 and 2 M, respectively. Since the electrode is uncharged, the anion and cation profiles are identical. Hence, we plot only the average concentration profile normalized to one, $c(x)/c(\infty) = [c_+(x) + c_-(x)]/[2c(\infty)]$, in these figures. For all three concentrations, the GC profile would be $c(x) = c(\infty)$, i.e. a straight line, whose value is unity, in each of the figures. The results for Model 80|80|80 (no dielectric boundaries) show the consequences of ion size, a parameter missing in the GC theory. For Model

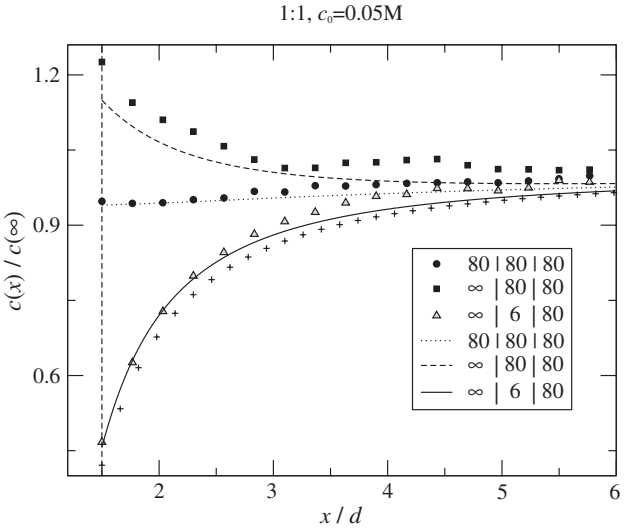

Figure 3. Density profiles of a 0.05 M 1:1 electrolyte near an uncharged electrode. The symbols and the curves correspond to Monte Carlo and theoretical results, respectively, for the various models as indicated in the figure, while the plus signs are theoretical results for the 6|6|80 model. The theoretical curves have been calculated from equation (22).

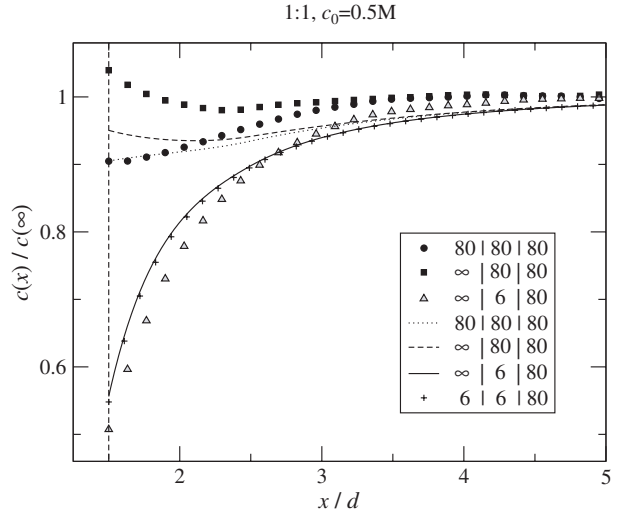

Figure 4. Density profiles of a 0.5 M 1:1 electrolyte near an uncharged electrode. The symbols and curves have the same meaning as in figure 3.

80|80|80, the contact value of $c(x)$ is proportional to the bulk pressure, p, through the *exact* contact value theorem [19],

$$\rho(3d/2)k_{\mathrm{B}}T = p, \tag{8}$$

where $\rho(x)$ is the total number density profile of the ions at x, which is proportional to $c(x)$, and p is the pressure of the bulk electrolyte. The physical content of equation (8) is that, for Model 80|80|80, the momentum

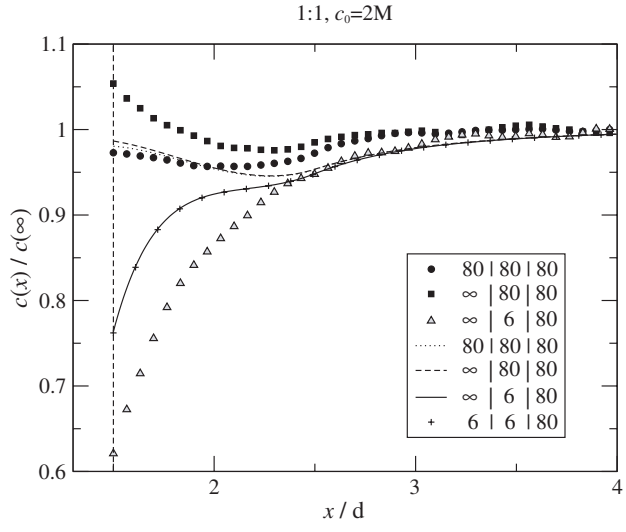

Figure 5. Density profiles of a 2 M 1:1 electrolyte near an uncharged electrode. The symbols and curves have the same meaning as in figure 3.

transfer at the distance of closest approach is equal to the bulk pressure. We know of no exact analogues of equation (8) for Models ∞|80|80, ∞|6|80 and 6|6|80. Equation (6) is satisfied by the GC theory. However, in the GC theory the ions are points and the ideal gas result for the pressure applies. Thus, in the GC theory, $p = \rho(\infty)k_{\mathrm{B}}T$ and $\rho(x) = \rho(\infty)$. In reality, the pressure includes not only the direct effect of the excluded volume of the ions, a positive contribution, but also the effect of the Coulombic interactions among the ions, a negative contribution, with the result that, for the conditions considered here, the pressure of the electrolyte is less than the ideal gas pressure. Hence, the concentration profile for Model 80|80|80 decreases as x approaches contact at $3d/2$. That is, $\rho(3d/2) = p/k_{\mathrm{B}}T$, but $p/k_{\mathrm{B}}T < \rho(\infty)$. Hence, even before dielectric boundaries are taken into consideration, the GC profiles are somewhat too large near contact. In figure 5, where the concentration is high (2 M), the profile goes through a minimum near contact, indicating that the hard core effect is becoming more important for 2 M and is counteracting at short range the longer range coulombic term; volume exclusion makes the ions crowd near the surface, while the attraction between ions in the diffuse layer draws ions away from the electrode.

Next, the effect of the metallic nature of the electrode is considered in Model ∞|80|80. Intuitively one might think that, since 80 is very large for a dielectric coefficient, there would be little difference between Models 80|80|80 and ∞|80|80. However, as is seen in figures 3–5, each ion induces a charge of the opposite sign on the surface of the electrode. Consequently, the ions are attracted to the electrode. This attraction is

strong enough to overcome the decrease in $c(x)$ due to the Coulomb forces between the ions, and $c(3d/2) > c(\infty)$ for Model $\infty|80|80$.

Next we consider Model $\infty|6|80$ in figures 3–5. For this model, there is a repulsive force due to the induced charge on the dielectric interface at δ. This is stronger than any attractive force due to the induced charge at the electrode and therefore $c(3d/2)$ is strongly reduced.

Results for a 2:2 electrolyte at a bulk concentration of 0.5 M are shown in figure 6. The reduction in $c(x)$ is even more pronounced than that in figure 4; even the $\infty|80|80$ curve shows drying at the interface. The Coulomb forces among the ions are stronger, as are the attractive forces due to the induced charge which are proportional to z_i^2.

Finally, results for a 2:1 electrolyte for a bulk concentration of 0.5 M are reported in figure 7. Since the charges of the ions are not symmetric, the concentration profiles of the anions and cations differ. In figure 7, the profile for each ionic species is normalized by its own bulk value $c_i(\infty)$. Figure 7 shows that the monovalent ions approach the electrode somewhat more closely than the divalents. There is also a slight maximum in the divalent ion profile, but this is a small effect. We have verified that the area of the difference in the monovalent and divalent profiles is zero to within the accuracy of our simulation. Thus, there is no net charge on the electrode (apart from polarization charges) or within the ion profiles. However, the asymmetry of the profiles means that, as is seen in the inset of figure 7, there is a non-zero electrostatic potential even though the electrode is uncharged. We defer further discussion of the potential to a later paper where we will examine the charge–potential characteristics for both charged and uncharged electrodes.

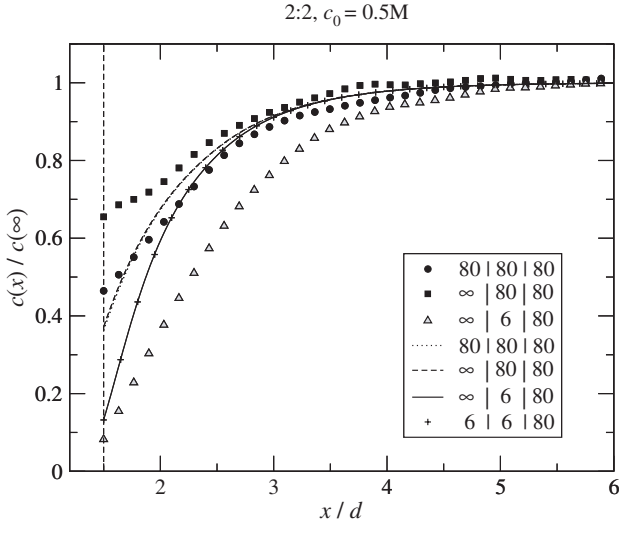

Figure 6. Density profiles of a 0.5 M 2:2 electrolyte near an uncharged electrode. The symbols and curves have the same meaning as in figure 3.

5. Electrostatics of the $\epsilon_1|\epsilon_2|\epsilon_3$ model

We have already noted that for Model $\infty|6|80$ the repulsive effect of the induced charge at the 6|80 dielectric interface at $x = \delta = d$ exceeds the attractive effect of the induced charge at the $\infty|6$ interface at $x = 0$. We have made some simulations for Model 6|6|80 for a 1:1 electrolyte whose concentration is 0.5 M and

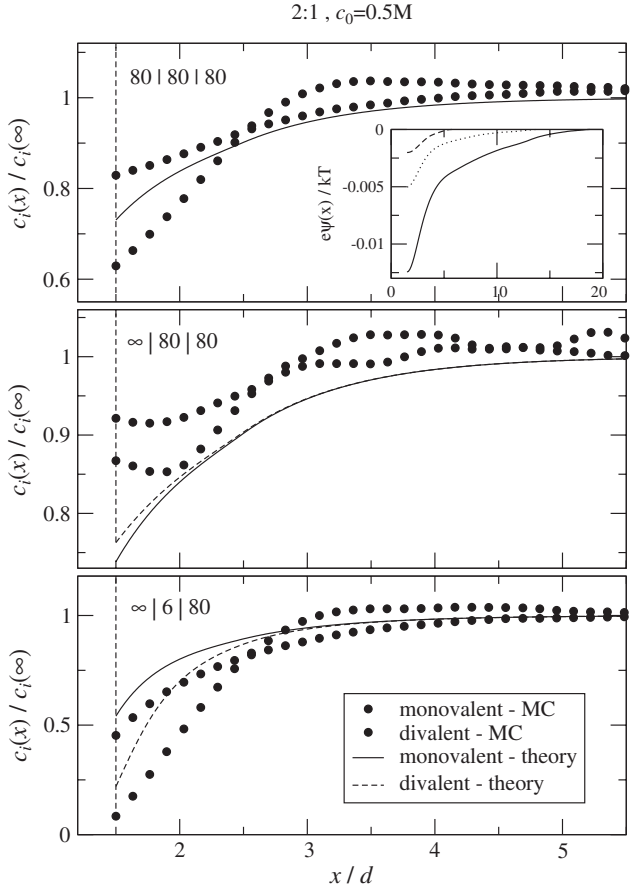

Figure 7. Normalized density profiles of a 0.5 M 2:1 electrolyte near an uncharged electrode. The three insets show results for the three different geometries (80|80|80, $\infty|80|80$ and $\infty|6|80$). The symbols and the curves correspond to Monte Carlo and theoretical results, respectively, for the two ionic species as indicated in the figure. The theoretical cation and anion profiles are identical for the 80|80|80 model. The profiles for the $\infty|6|80$ and 6|6|80 models are indistinguishable. The inset shows the MC potential profiles; the dotted, dashed and solid lines denote 80|80|80, $\infty|80|80$ and $\infty|6|80$ results, respectively.

for a 2:1 electrolyte whose concentration is 0.5 M. In both cases, their results are virtually identical to those of Model $\infty|6|80$. For this reason, we have not plotted the MC results for the 6|6|80 geometry in figures 4 and 7. This does not mean that there is no value in simulations with multiple dielectric interfaces. Indeed, since the above result is not intuitively obvious, this observation illustrates the value of our method. There is no reason to expect that the $\infty|6|80$ and the 6|6|80 models would be equivalent for all concentrations, all ion diameters, and all electrode charges.

In order to gain more insight into this result, we give below the solution of Poisson's equation for a single charge in region 3 of the $\epsilon_1|\epsilon_2|\epsilon_3$ model and obtain a generalization of the well known 'image' result for a single dielectric boundary. Smythe [20] presents an elegant method for solving Poisson's equation for this problem and gives results for the potential in region 1 for a $1|\epsilon|1$ model. Adapting Smythe's method to our problem, we find that, in Fourier Bessel (k) space, the response potential in region 3 for the $\epsilon_1|\epsilon_2|\epsilon_3$ model with the $\epsilon_1|\epsilon_2$ and $\epsilon_2|\epsilon_3$ boundaries located at $x=0$ and $x=\delta$, respectively, and a unit charge located in region 3 at $x_0 > \delta$ is given by

$$\Phi(k) = \left\{\frac{\epsilon_3-\epsilon_2}{\epsilon_3+\epsilon_2} - \frac{4\epsilon_2\epsilon_3}{\epsilon_3^2-\epsilon_2^2}\left[\frac{1}{1-\alpha\,\exp[-k(2\delta)]}-1\right]\right\} \times \exp[-k(x_0-2\delta)], \tag{9}$$

where

$$\alpha = \frac{(\epsilon_1-\epsilon_2)(\epsilon_3-\epsilon_2)}{(\epsilon_1+\epsilon_2)(\epsilon_3+\epsilon_2)}. \tag{10}$$

If $\epsilon_1=\epsilon_2$, $\alpha=0$ and the second term on the right of equation (9) vanishes, giving the usual 'image' result for a $\epsilon_2|\epsilon_3$ discontinuity at $x=\delta$. If $\epsilon_2=\epsilon_3$, the first term on the right of equation (9) vanishes. Superficially, one might think that the zero in the denominator of the coefficient of the second term on the right of equation (9) is a concern. However, if the fraction in the second term is expanded as a power series in α, all the terms, except the term in α, vanish and $\alpha(\epsilon_3^2-\epsilon_2^2)^{-1}$ is finite in the limit $\epsilon_2 \to \epsilon_3$. Consequently, the usual 'image' result for a $\epsilon_1|\epsilon_2$ discontinuity at $x=0$ is obtained. Also the correct limits are obtained in the limits of large and small δ. For δ large, the second term on the right of equation (9) vanishes. For $\delta=0$, the term in the square brackets is $\alpha/(1-\alpha)$. The sum of the first and second terms on the right of equation (9) gives the correct result.

After the completion of this work we found that a result equivalent to equation (9) has been given by Carnie and Chan (C^2) [21] in the context of a slab surrounded by an electrolyte. Also, it has been pointed out to us that Bell and Levine (BL) [22] have examined a three slab model consisting of an electrolyte, an inner layer and an electrode, which is similar to the one considered here and we expect that equation (9) is implicit in their work.

The potential in x space can be obtained by integrating this result. However, it is more convenient to expand the denominator as a power series in α and then invert analytically. The result for a unit charge at $x_0 > \delta$ and $y_0 = z_0 = 0$ is

$$\phi_3(x,y,z) = \frac{1}{r} + \left(\frac{\epsilon_3-\epsilon_2}{\epsilon_3+\epsilon_2}\right)\frac{1}{[y^2+z^2+(x_0-2\delta+x)^2]^{1/2}} - \frac{4\epsilon_2\epsilon_3}{\epsilon_3^2-\epsilon_2^2}\sum_{n=1}^{\infty}\frac{\alpha^n}{[y^2+z^2+(x_0-2\delta+2n\delta+x)^2]^{1/2}}, \tag{11}$$

where $r=[(x-x_0)^2+y^2+z^2]^{1/2}$.

So why are the Model 6|6|80 and Model $\infty|6|80$ results so similar for $\delta = 3$ Å? Stated another way, why does a 3 Å dielectric slab behave as if it were infinitely thick? This is not an intuitive result. If we examine the terms in equation (11) numerically, we find that if δ, the thickness of the ϵ_2 region, is exceedingly small or exceedingly large, the expected results are obtained. However, if we start with δ large and then allow δ to decrease, the contribution of the third term increases in magnitude and for $\delta = 3$ Å becomes comparable in magnitude to the second term, but is nearly independent of x. Thus, the 6|6|80 and $\infty|6|80$ results are similar not because the third term in equation (11) is small, but because its derivative is small; it is differences in energy rather than absolute values of energy that are significant. As δ is decreased further, the second term becomes small (and flatter) and the derivative, as well as the magnitude, of the third term becomes appreciable.

Bell and Levine have also noted that the effect of an inner layer with a low dielectric coefficient is to reduce the metallic behaviour of the electrode.

6. Simple expression and results

We can use the result of the previous section to develop a simple expression for the concentration profiles of our system. First, let us consider a $\epsilon_3|\epsilon_3|\epsilon_3$ model. We know that for such a model at contact

$$\sum_i c_i(3d/2)/c_i(\infty) = \sum_i \rho_i(3d/2)/\rho = p/\rho k_B T, \tag{12}$$

where $\rho_i(x)$ is the density profile of the ions of species i, $\rho = \sum_i \rho_i$ and $\rho_i = \rho_i(\infty)$. Equation (12) is useful only if the pressure p is known. Fortunately, the mean spherical

approximation (MSA) yields an expression for p that is accurate for all but the largest values of q^*. This result is

$$\frac{p}{\rho k_B T} = a = a_0 - \frac{\Gamma^3}{3\pi\rho}, \tag{13}$$

where

$$a_0 = \frac{1+\eta+\eta^2-\eta^3}{(1-\eta)^3}, \tag{14}$$

$\eta = \pi\rho d^3/6$,

$$\Gamma = \frac{1}{2d}\left((1+2\kappa d)^{1/2} - 1\right) \tag{15}$$

and

$$\kappa^2 = \frac{4\pi\beta e^2}{\epsilon}\sum_i z_i^2 \rho_i. \tag{16}$$

κ is the usual Debye–Hückel parameter and $\beta = 1/k_B T$. Recall that $\epsilon = \epsilon_3$ is the dielectric coefficient of the region (region 3) that contains the ions. Note that a is the difference between a repulsive uncharged hard-sphere term, a_0, and an attractive electrostatic term. Whether a is positive or negative depends on the relative magnitudes of these two terms. In a theory that is more general than the MSA, it is likely that these two contributions to a would not be decoupled. Although approximate, equation (13) is satisfactory for our purposes.

This gives us a useful expression for the contact value. However, we still need the x dependence of the concentration profiles. Here again, the MSA provides some guidance. In the MSA,

$$\frac{c_i(x)}{c_i(\infty)} = \begin{cases} g_0(x-3d/2), & \text{for } x > 3d/2, \\ 0, & \text{for } x < 3d/2, \end{cases} \tag{17}$$

where $g_0(t)$ is a function that Smith and Henderson [23] have given explicitly for $t < 6d$. Note that the above MSA result is defective in at least two regards. First, it is independent of the ion species and charge. Thus, at best $g_0(0)$ can only be an approximation to a_0. Second, even for this charge-independent part of p, the MSA is inexact. Instead of a_0, the MSA contact value is $(1+2\eta)/(1-\eta)^2$, which is the MSA value for the compressiblity, $\beta\partial p/\partial\rho$, for *uncharged* hard spheres. This agrees with a_0 only for small η. Even so, we can use this MSA result to construct an expression for x dependence of the charge-independent part of the concentration profile. It is plausible that the x dependence of the second term is given by the usual PB expression, $\exp(-\kappa x)$. Thus, we obtain for a $\epsilon_3|\epsilon_3|\epsilon_3$ model,

$$\frac{c_i(x)}{c(\infty)} = \frac{c_0(x)}{c_0(\infty)} = 1 + (a_0 - 1)\frac{(1-\eta)^2}{1+2\eta}[g_0(x-3d/2) - 1] - \frac{\Gamma^3}{3\pi\rho}\exp[-\kappa(x-3d/2)], \tag{18}$$

and, as in equation (17), $c_i(x) = 0$ for $x < 3d/2$. That is, we have divided $g_0(x-3d/2) - 1$ by its (incorrect) MSA contact value and then multiplied by its correct (or at least more correct) hard sphere contact value. We use $g_0(x-3d/2) - 1$ rather than $g_0(x-3d/2)$ so that the right-hand side of equation (18) equals 1 at large x. Note that equation (18) assumes that $c_i(x)$ is independent of species if the electrode is uncharged and if there are no dielectric boundaries. This seems correct for symmetric salts, but, as is seen in figure 7, is not correct for asymmetric salts, even if they all have the same diameter. To obtain the species dependence would require a contact value theorem for each species. This we do not have. Equation (12) is a theorem for the sum of contact values. To the extent that within a $\epsilon_3|\epsilon_3|\epsilon_3$ model $c_i(x)$ is independent of species, equation (18) satisfies equations (12) and (13).

This result is compared with some of our simulation results for an uncharged electrode with no dielectric boundaries in figures 3–7. The results are quite reasonable for figures 3–6 where $z_1 = -z_2$ but fails to give the species dependence seen in figure 7. Equation (18) has captured the essence of the simulation results for symmetric salts at an uncharged electrode with no dielectric boundaries.

We now turn our attention to the effect of dielectric boundaries. Onsager and Samara (OS) [11] have described a simple theory for the concentration profiles of a $\epsilon_1|\epsilon_2$ dielectric boundary $x = 0$ (with the charges confined to region 1). Their result, a screened self-image expression, is

$$\ln\left[\frac{c_i(x)}{c_i(\infty)}\right] = -\frac{\beta z_i^2 e^2}{4\epsilon_1 x}\left(\frac{\epsilon_1 - \epsilon_2}{\epsilon_1 + \epsilon_2}\right)\exp[-2\kappa x]. \tag{19}$$

Subsequent to the work of OS, this result has been obtained by BL, Nicholls and Pratt (NP) [24], Outhwaite [25] and C^2. The method of C^2 is best known to us and probably the most general. The work of C^2 together with the comment of Henderson and Plischke [26] shows that the OS result follows from a fully self-consistent solution of a second-order inhomogeneous linearized PB equation (in k space) for a flat uncharged electrode.

The results of NP and C^2 were obtained in k space and involve the function

$$\bar{\Delta}(k) = \frac{\epsilon_2 p - \epsilon_1 k}{\epsilon_2 p + \epsilon_1 k}, \tag{20}$$

where $p = (\kappa^2 + k^2)^{1/2}$. Equation (19) results from integration of the k space result of NP and C^2 only if $\bar{\Delta}(k)$ is independent of k. This raises the question of whether we should base our expression on the original OS x space result or the NP and C^2 k space result. Reference to figure 2 of C^2 shows that the effect of the k dependence of $\bar{\Delta}(k)$ is to account in part for the electrostatic contribution to the contact value that is missing in the OS theory. Indeed, if the k dependence of $\bar{\Delta}(k)$ is taken into account then, in the absence of a dielectric boundary, the contact value would be

$$\ln\left[\frac{c_i(3d/2)}{c_i(\infty)}\right] = -\frac{1}{6}\left(\frac{\beta z_i^2 e^2}{\epsilon_3 d}\right)\kappa d, \tag{21}$$

which is just the low concentration version of equation (13). That is, we can obtain the low concentration version of the $\epsilon_3|\epsilon_3|\epsilon_3$ model contact value either by integrating $\bar{\Delta}(k)$ or from equation (13). We prefer equation (13) because it is not limited to low concentrations, it is easier to use, and the generalization to the $\epsilon_1|\epsilon_2|\epsilon_3$ model is more straightforward.

Our result for the $\epsilon_1|\epsilon_2|\epsilon_3$ model is an obvious extension of the OS result and is

$$\ln\left[\frac{c_i(x)}{c_i(\infty)}\right] = \ln\left[\frac{c_0(x)}{c_0(\infty)}\right] - \frac{\beta z_i^2 e^2}{4\epsilon_3(x-\delta)}\left(\frac{\epsilon_3 - \epsilon_2}{\epsilon_3 + \epsilon_2}\right) \times \exp\left[-2\kappa(x-\delta)\right] + \beta z_i^2 e^2\left(\frac{\epsilon_2}{\epsilon_3^2 - \epsilon_2^2}\right) \times \sum_{n=1}^{\infty} \frac{\alpha^n}{x - \delta + n\delta} \exp\left[-2\kappa(x - \delta + n\delta)\right] \tag{22}$$

for $x > 3d/2$ and $c_i(x) = 0$ otherwise. Equation (22) reduces to the OS result if $\epsilon_1 = \epsilon_2$ or $\epsilon_2 = \epsilon_3$, if $c_0(x) = 1$, and if δ is small or large. When using equation (22), we summed 100 terms in the series. In most cases, a smaller number of terms is sufficient.

Some results of equation (22) are shown in figures 3–6 for Models $\infty|80|80$, $\infty|6|80$ and $6|6|80$. The agreement with the simulation results is fairly reasonable for 1:1 salts at 0.05 M, but less so for 0.5 and 2 M, and when divalent ions are present. A small difference between Model $\infty|6|80$ and Model $6|6|80$ is noticeable at 0.05 M, but there is no appreciable difference at higher concentrations. In both the simulations and theory the difference between Model $\infty|80|80$ and $80|80|80$ decreases as the concentration increases. However, equation (22) exaggerates this tendency. Generally speaking, the profiles that result from equation (22) decay too rapidly. At high concentrations, the simulation profiles show oscillations. It is tempting to replace the PB exponentials, $\exp(-\kappa t)$ by the MSA function, $f(t)$. The MSA function tends to the PB exponential at low concentrations and small $z_i^2 q^{*2}$, but can exhibit oscillations at larger values of these quantities because of the presence of spherical Bessel functions. However, these oscillations are weaker than those seen in the simulations so we have not pursued this.

Results for the unsymmetric 2:1 case are plotted in figure 7. Even for the $80|80|80|$ model, the simulation results show a different profile for the monovalent and divalent salts which is not predicted by equation (22). However, equation (22) seems to describe qualitatively the effect of the dielectric boundaries even in the 2:1 case. We note that the simulation profiles show oscillations that are lacking in equation (22). Curiously, in the $\infty|80|80$ geometry, the MC monovalent profile is larger than the MC divalent profile near contact whereas the theoretical results show the opposite behaviour.

7. Conclusions

In the simulations reported here, there is no source charge on the electrode. On average, there is no induced charge on the dielectric interfaces for the 1:1 and 2:2 cases. Nonetheless, the concentration profiles of the ions are affected by the induced charges. Although on average there is no induced charge, there is a non-uniform net charge on the dielectric interfaces at *every instant* of the simulation. It is this instantaneous induced charge that is the cause of the behaviour of the profiles. Although the induced charges are instantaneously non-uniform, the average induced charge is uniform (and zero) and the ion profiles are functions only of x.

As far as the 2:1 case is concerned, the dipole layer seen in figure 7 results in a net average polarization charge on the dielectric boundaries. The monovalent ions that are closer to the interface on average induce a higher (in magnitude) polarization charge on average than the divalent ions.

We have already noted that for Model $\infty|6|80$ the repulsive effect of the induced charge at the $6|80$ dielectric interface at $x = \delta$ exceeds the attractive effect of the induced charge at the $\infty|6$ interface at $x = 0$. However, the $\infty|6|80$ and $6|6|80$ models can only be equivalent if δ is large in some sense. We have examined Poisson's equation for a single charge at a more general

two dielectric boundary problem in order to understand this question. We note that there is nothing in nature that requires dielectric interfaces to be far apart. In fact, the reverse is true. We expect that in the inner layer the dielectric coefficient decreases continuously from 80 to a small value, perhaps even unity, with something like 6 being only the average value. This could be modelled by a series of closely spaced dielectric interfaces.

Our simulations do not support the popular idea that a theory or simulation of the diffuse layer can be combined with a treatment of the inner layer and/or the electrode that involves dielectric boundaries unless one takes into account the fact that the diffuse layer profiles are affected by the induced charge at these boundaries.

Although the simulations that we report were made using the method of Boda *et al*., equation (11) may permit faster simulations for planar boundaries than can be made using the Boda *et al*. method, this does not detract from the usefulness of the Boda *et al*. method as this method can be used with *arbitrary* (fixed) boundaries.

If the use of the GC theory, with or without a dielectric interface, is suspect, what should one do? A simple analytic result is an undeniable convenience, and, for the moment, computer simulation does not seem useful for routine analysis of experiment. As computer power continues to increase and computer cost continues to decrease, however, in the future this will become less and less of a consideration. Most theories are not able to take the induced charge at a dielectric interface into account. Exceptions are the pair integral equation of Plischke and Henderson [27] and Kjellander and Marcelja [28] that can be adapted to account for induced charge at dielectric boundaries, but are computationally intensive. The methods of Croxton *et al*. [29], based on the BBGY hierarchy, and the cluster-perturbation theory of Vertenstein and Ronis [30] are worth pursuing. The modified Poisson–Boltzmann (MPB) theory [31], which is based on the work of BL, is a comparatively simple theory that can account for induced charge at a single planar dielectric interface. The authors do not know whether the MPB theory can be adapted to a general inhomogeneous dielectric interface, but suspect that it can if equation (11) and its generalizations are used. If this can be done, the MPB approach is worth pursuing. Also, Fawcett and Henderson [32] have had good success with modifying the GC theory semi-empirically in light of simulations. Perhaps this approach can be extended to include induced charge. Tests of any theory must consider 2:1 electrolytes because the charge reversal observed there offers the greatest challenge. This phenomena is not described even qualitatively by the OS theory.

In summary, we believe that it is important to include the dielectric interfaces both at the inner–diffuse layer boundary and at the electrode. Multiple dielectric interfaces may be even more important. Obviously, there is much to be done.

Acknowledgement

The authors are pleased to acknowledge the fact that without the encouragement and help of Wolfgang Nonner and Bob Eisenberg this work would not have been completed. This work was supported in part by a NATO Collaborative Linkage Grant (PST. CLG.980366).

References

[1] G. Gouy. *J. phys. (France)*, **9**, 457 (1910).
[2] D.L. Chapman. *Phil. Mag*., **25**, 475 (1913).
[3] W. Schmickler, D. Henderson. *Prog. Surf. Sci*., **22**, 323 (1986).
[4] G.M. Torrie, J.P. Valleau. *J. chem. Phys*., **73**, 5807 (1980).
[5] G.M. Torrie, J.P. Valleau, G.N. Patey. *J. chem. Phys*., **76**, 4615 (1982).
[6] G.M. Torrie, J.P. Valleau. *J. phys. Chem*., **86**, 3251 (1982).
[7] J.P. Valleau, G.M. Torrie. *J. chem. Phys*., **81**, 6291 (1984).
[8] D. Boda, D. Henderson, K.-Y. Chan, D.T. Wasan. *Chem. Phys. Lett*., **308**, 473 (1999).
[9] D. Boda, W.R. Fawcett, D. Henderson, S. Sokolowski. *J. chem. Phys*., **116**, 7170 (2002).
[10] D. Boda, D. Henderson, P. Plaschko, W.R. Fawcett. *Molec. Sim*., **30**, 137 (2004).
[11] L. Onsager, N.N.T. Samara. *J. chem. Phys*., **2**, 528 (1934).
[12] D. Boda, D. Gillespie, W. Nonner, D. Henderson, B. Eisenberg. *Phys. Rev*. E, **69**, 046702 (2004).
[13] R. Allen, J.P. Hansen, S. Melchionna. *Phys. Chem. Chem. Phys*., **3**, 4177 (2001).
[14] C.S. Pomelli, J. Tomasi, V. Barone. *Theor. Chem. Acc*., **105**, 446 (2001).
[15] H. Hoshi, M. Sakurai, Y. Inoue, R. Chûjô. *J. chem. Phys*., **87**, 1107 (1987).
[16] J. Lu, M.E. Green. *Progr. Colloid Polym. Sci*., **103**, 121 (1997).
[17] M.E. Green, J. Lu. *J. phys. Chem*. B, **101**, 6512 (1997).
[18] J. Lu, M.E. Green. *J. phys. Chem*. B, **103**, 2776 (1999).
[19] D. Henderson, L. Blum, J.L. Lebowitz. *J. electroanal. Chem*., **102**, 315 (1979).
[20] W.R. Smythe. *Static and Dynamic Electricity*, pp. 182–184, McGraw-Hill, New York (1950).
[21] S.L. Carnie, D.Y.C. Chan. *Molec. Phys*., **51**, 1047 (1984).
[22] G.M. Bell, S. Levine. *J. colloid Interface Sci*., **41**, 275 (1972).
[23] W.R. Smith, D. Henderson. *Molec. Phys*., **19**, 411 (1970).
[24] A.L. Nicholls III, L.R. Pratt. *J. chem. Phys*., **76**, 3782 (1982); *ibid*., **77**, 1070 (1982).

[25] C.W. Outhwaite. *J. chem. Soc. Faraday II*, **79**, 1315 (1983).
[26] D. Henderson, M. Plischke. *Molec. Phys.*, **62**, 801 (1987).
[27] M. Plischke, D. Henderson. *J. chem. Phys.*, **88**, 2712 (1988).
[28] R. Kjellander, S. Marcelja. *J. chem. Phys.*, **82**, 2122 (1985).
[29] T. Croxton, D. McQuarrie, G. Patey, G. Torrie, J. Valleau. *Can. J. Chem.*, **59**, 1998 (1981).
[30] M. Vertenstein, D. Ronis. *J. chem. Phys.*, **87**, 4132 (1987).
[31] C.W. Outhwaite, L.B. Bhuiyan. *J. chem. Soc. Faraday Trans.*, **79**, 707 (1983).
[32] W.R. Fawcett, D. Henderson. *J. phys. Chem.* B, **104**, 6837 (2000).